Collaborative Operation and Real-Time Control of Roller Fleet for Asphalt Pavement Compaction

Donghai Liu[a] , Junjie Chen[a], Shuai Li[b]

[a] State Key Laboratory of Hydraulic Engineering Simulation and Safety, Tianjin University, 135 Yaguan Road, Tianjin 300350, China

[b] Department of Civil and Environmental Engineering, the University of Tennessee, Knoxville, 851 Neyland Dr. Knoxville, TN, the United States

This is the peer-reviewed post-print version of the paper:
Liu, D., Chen, J., & Li, S. (2019). Collaborative Operation and Real-Time Control of Roller Fleet for Asphalt Pavement Compaction. *Automation in Construction*, 98: 16-29. Doi: 10.1016/j.autcon.2018.11.005.
The final version of this paper is available at: https://doi.org/10.1016/j.autcon.2018.11.005.
The use of this file must follow the Creative Commons Attribution Non-Commercial No Derivatives License, as required by Elsevier's policy.

Abstract

Compaction is one of the most critical processes in the asphalt pavement construction. Collaborative control of multiple rollers in the construction site to enable each roller to compact the right position at the right time with the right compaction parameters to ensure compaction quality is an unaddressed challenge. There are three technical barriers, i.e. how to collect and communicate compaction data of each roller, how to aggregate the collected data to determine compaction parameters, and how to control the roller fleet based on the real-time compaction parameters. To address the technical barriers, a cyber-physical system is designed and implemented. A framework is proposed for multi-roller compaction monitoring, which consists of five modules, i.e. data acquisition module, data transmission module, remote servers, in-situ control module, and monitoring terminal. Algorithms are created to calculate compaction parameters in the scenario of multi-machine operations. A managerial

mechanism involving cyber space, human intervention, and compaction machines is set up to achieve collaborative compaction control. Field experiments were conducted to validate the efficacy of the system, of which the results suggest the proposed system can effectively control the compaction process. With inappropriate compaction effort being identified, tracked, and rectified in real time, the compaction quality is ensured. The development of the cyber-physical system paves the way for deploying multiple automatic rollers in the construction site for collaborative and adaptive compaction.

Keywords: Asphalt pavement; Quality control; Intelligent compaction; Cyber-physical system; Multi-roller collaboration; Real-time control.

1. Introduction

Compaction is a vital process in the construction of asphalt pavement. Multiple rollers are operated to accelerate the compaction of asphalt pavements that have long mileages and wide cross-sections to meet tight construction schedules. The roller fleet comprises different types of compacting machines, such as steel-wheel compactor and rubber tyre roller. The compaction process typically involves three operation stages [1], i.e. the initial rolling, the repeated rolling, and the final rolling. Each stage has specific requirements for roller type (steel-wheel or rubber tyre), operation mode (static or vibratory), and compaction parameters (vehicle speed, overlap distance, etc.). Noncompliance with these requirements may lead to unqualified compaction results, which will result in ruts, cracking, and raveling, and thus reduce the pavement service life.

Under the current practice, quality control for multi-roller asphalt compaction relies on traditional methods such as on-site supervision during compaction and random spot test after compaction, which not only are time-consuming and labor-intensive, but also yield unreliable results with limited coverage. With advancements in intelligent compaction (IC) technologies, wireless communication technologies, feedback control, and data analytics, cyber-physical systems have been developed that provide a new means to control the compaction parameters such as excitation force, roller passes and vehicle speed, and to monitor and visualize the compaction quality [2-6]. Kassem et al. [3] developed a compaction monitoring system (CMS) for asphalt mixtures by integrating a global positioning system (GPS) and various sensors, which can provide the roller operator with real-time color displays of roller passes,

compaction effectiveness, and temperature. Xu and Chang [4] proposed a material-machine-information-human decision integrated system for adaptive quality control and acceptance of asphalt pavement, in which the collected material responses are used to optimize compaction efforts. To synchronize compaction information among different project stakeholders, Liu et al. [5] developed a real-time quality monitoring system to disseminate the monitored compaction parameters (i.e. roller trajectory, rolling passes, compacted elevation and compacted thickness) to operators, contractors, supervisors, and owners.

However, these cyber-physical systems fall short of coordinating multiple rollers in the compaction process. The operation information cannot be shared among different rollers during the construction. The data analysis can only be conducted after the compaction when the data from different machines are gathered in a manual way (e.g. use a USB to copy data from the on-board display) [7]. Thus, the analysis results cannot be obtained and fed back to the construction site in real time, which delays the identification of unqualified compaction operation, leading to an increase in construction cost brought by subsequent restoration work. Hence, existing technologies are not applicable in the real-time control and coordination of roller fleet under the complicated multi-roller compaction process. To fill in the gap of current practice, a quality control method for asphalt pavement compaction is proposed in this study that can coordinate multi-roller operations and realize real-time control of compaction quality.

2. Review of relevant studies

The literature review has been primarily conducted to determine the key factors that affect the compaction quality in multi-roller scenario from the perspective of compactness, roughness, and uniformity.

2.1. Control of compactness

IC uses a material stiffness index — defined as IC measurement value (ICMV) — to represent pavement compactness. There are primarily two types of ICMV: (1) unitless indexes derived from the harmonic component analysis, e.g. CMV (compaction meter value) [8], CCV (compaction control value) [9], and THD (total harmonic distortion); (2) dimensional indexes derived from the roller-soil interaction model, e.g. E_{vib} [10], k_B [11], and MDP (machine drive power). To investigate the applicability of these indexes, numerous researches have been carried out to study the correlation between ICMV and spot test measurements, as listed in Table 1. The correlation between ICMV and conventional spot test results is affected by many factors (e.g. distribution of materials, stiffness of sub-layers, influence depth, and data analysis method), and thus using ICMV to represent the compactness may cause biases in some projects. As a result, before the characterization mechanism of ICMV is further revealed, real-time control of compaction parameters such as roller passes, excitation force, and vehicle speed, is still vitally important for achieving better compactness.

2.2. Control of roughness

The control of compaction sequence is critical to meet the roughness requirement. Pavement

compaction is performed by a combination of different rollers in a certain sequence [1]. For example, the compaction procedure of asphalt surface layer includes three stages, i.e. the initial rolling, the repeated rolling, and the final rolling. The purpose of initial rolling is to smooth the pavement surface and make the compacted materials reach a certain level of strength immediately after paving. In this stage, 2 to 4 times of rolling by steel-wheel compactor in static mode are recommended. Followed by the initial rolling, the compactness and strength of the pavement are significantly improved in the repeated rolling stage. The kneading action by rubber tyre rollers and (or) the vibratory rolling by steel-wheel compactors with high frequency are required in this stage. Thereafter, the final rolling is performed to eliminate the ruts produced by rubber tyre rollers or vibratory rollers. In the final rolling stage, at least 4 times of rolling by steel-wheel compactors in static mode are required.

Shi et al. [18] points out that the implementation of the aforementioned rolling sequence is critically vital for the assurance of pavement roughness. Noncompliance with the required compaction sequence results in uneven settlement and pavement ruts. In current practice, the straightedge or the continuous evenness device is used to assess the roughness after compaction. Chen et al. [19] and Loizos and Plati [20] integrated the state-of-the-art sensors to measure pavement roughness. Since the roughness is evaluated after compaction in these researches, it will cost a lot to perform the restoration work after the flaws are detected. Before compaction, the paving thickness and flatness are measured by a balance beam instrumented on the paver. Liu et al. [21] and Walters et al. [22] investigated the real-time

monitoring method of asphalt paving by using LiDAR, total station and other sensors, which can be utilized to control paving thickness and roughness. However, even though the paving process is under strict control, some quality issues such as ruts are still likely to emerge afterwards once the rolling sequence is not executed correctly during compaction. Therefore, there is a critical need to monitor the rolling sequence during pavement compaction.

2.3. Control of uniformity

Xu and Chang [4] established a regression model that used ICMV to predict dry density, and the standard deviation (or covariance) was used to reflect the uniformity. Vennapusa et al. [23] and Xu et al. [24, 25] used semivariogram based geo-statistical analysis to characterize and quantify non-uniformity of compacted materials. However, all these methods are post-compaction assessments, which cannot provide necessary information for real-time control of the compaction process.

Overlap distance is one of the essential compaction parameters that affect the uniformity [24, 25] of asphalt pavement. With the purpose of achieving a high bonding strength between compaction strips, the adjacent strips should overlap each other at the transverse edges (e.g. in the stage of repeated rolling, 100~200 millimeters of overlap distance is required). Noncompliance with this requirement leads to weak areas in the adjacent regions between different strips, where the compactness is lower than the overall level of the entire construction zone. Hence, overlap distance between strips should be monitored during the compaction process to ensure uniformity.

To sum up, roller passes, vehicle speed, excitation force, compaction sequence, and overlap distance are five key factors that influence the multi-roller compaction quality. This study aims to develop and validate a cyber-physical system that is capable of achieving collaborative and real-time control of the above five compaction parameters under the multi-machine situation. In dam construction, there are precedents for compaction parameter control of multiple rollers. Zhong et al. [26, 27] investigated the real-time monitoring method of compaction quality for core rock-fill dams, and developed a system that can monitor the compaction parameters. These researches provide useful references for this study.

3. Challenges for multi-roller compaction control

The realization of multi-roller compaction control needs to address the challenges of data communication, data analytics, and feedback control from the perspective of developing a cyber-physical system.

(1) Data communication among multi-machines

In multi-roller operation scenario, multiple machines may roll across the same pavement section. The calculation of compaction parameters such as roller passes, overlap distance, and vehicle speed depends on spatial-temporal analysis of the integrated multi-roller operation information (i.e. roller ID, position coordinates, and vibration status). For instance, the total roller passes of a certain location on the pavement is calculated by accumulating the roller passes exerted by different rollers. Hence, the primary challenge lies in how to construct a

framework involving hardware and software that can collect, integrate, and analyze the multi-roller information in real time.

(2) Determination of real-time compaction parameters

Computing the compaction parameters requires the analysis of spatial relationship among multiple rollers and the retrieval of historical compaction data. For example, in the calculation of overlap distance, the occupied area of a roller needs to be determined first, then the spatial relation between the occupied area and other compacted strips is analyzed, and finally the information of the identified adjacent strip is retrieved from the database for calculating the overlap distance. This data analytic process calls for concise algorithms and an efficient data storage structure, which is another challenge for real-time control of multi-roller compaction.

(3) Collaborative control of multi-machines

The third challenge lies in how to set up a managerial mechanism to ensure that the abnormal rolling operation can be identified and adjusted in real time, and realize the collaborative control of multi-machines. This mechanism should include several aspects: 1) control criteria setting; 2) data collection and analysis; 3) anomaly identification; 4) warning feedback; 5) illegal operation adjustment.

4. Research framework

Fig. 1 presents the overall research framework. First, methodology investigations are carried

out to address the three issues confronting multi-roller compaction control, i.e. data communication among multi-machines, determination of real-time compaction parameters, and collaborative control of multi-machines. The proposed solution for multi-machine compaction monitoring enables data communication from the perspective of software and hardware. Algorithms for compaction parameters calculation use the collected data from different rollers to calculate roller passes, overlap distance, vehicle speed, and excitation force in real time, providing a data basis for the collaborative control of multi-machine operation. The procedure for collaborative control sets up a managerial mechanism involving cyber space, human intervention, and physical machine to realize real-time control of compaction process. Based on these methods, a real-time compaction monitoring system is developed and applied to a real-world case, with the purpose of verifying its applicability.

5. Methodology

5.1. Solution for multi-machine compaction monitoring

Fig. 2 presents a framework for multi-roller compaction monitoring, which consists of five modules, i.e. data acquisition module (DAM), data transmission module (DTM), remote servers (RES), in-situ control module (ICM), and monitoring terminal (MOT).

(1) The DAM is comprised of a GPS positioning module and a CMV and vibration monitoring meter. The real-time kinematic (RTK) GPS positioning module is used to track the roller positions in real time with a centimeter-level precision. The CMV and vibration monitoring meter processes the acceleration data collected from the vibration drum in real

206 time to determine CMV and excitation force. In order to distinguish the data collected from
207 different rollers, the collected data are associated with the roller ID, and then sent to the
208 remote servers (RES) by the data transmission module (DTM).
209
210 (2) The DTM connects all in-situ rollers with the remote servers. It not only sends the roller
211 operation information (i.e. roller ID, coordinates, and excitation force) to the remote database
212 servers, but also receives the processed data (i.e. roller passes, vehicle speed, overlap distance
213 and warning messages) from the servers. In areas where the mobile communication is
214 available, a data transfer unit (DTU) is used to communicate with the RES via 3G/4G
215 networks. When the mobile communication is unavailable, ad hoc networks are set up to
216 transfer data in a local area network. In order to prevent possible loss of data packet and
217 ensure real-time transmission, the DTM is equipped with a data cache and is able to redial
218 automatically.
219
220 (3) The RES stores the data collected from multi-machines and dynamically analyzes the data
221 during the compaction process. Specifically, the application servers collectively process the
222 multi-roller operation information (i.e. roller ID, coordinates, and excitation force) to obtain
223 roller passes, overlap distance and vehicle speed for each roller in real time. The excitation
224 force is represented by frequency and amplitude, which are calculated in the DAM before
225 sent to the RES. The obtained compaction parameters are then compared with the pre-set
226 control criteria. When noncompliance is detected, the system will generate warning messages.
227 The aforementioned calculated results are fed back to the in-situ control module (ICM) and

the monitoring terminal (MOT).

(4) The ICM consists of a personal digital assistant (PDA) and an on-board display. Field supervisors use the PDA to receive warning messages and to coordinate roller operations. The on-board display presents the real-time compaction parameters and warning messages of a single roller to its operator for adjusting inappropriate compaction efforts timely.

(5) The MOT provides project owners and supervisors with a holistic overview of compaction process. Compaction trajectories of all rollers and corresponding compaction parameters are displayed on the screen; and a color-coded map is generated to visualize the roller passes of the whole construction zone. Users can export compaction reports as quality acceptance (QA) materials.

5.2. Algorithms for compaction parameters calculation

Fig. 3 illustrates the process for calculating compaction parameters in the scenario of multi-machine operations. The compaction process record is critical for multi-machine collaboration, because: (1) it helps a single roller to determine its current roller passes and the spatial relation with adjacent strips in the overall compaction process; (2) it needs to be updated by the calculated results for computation in the next cycle.

5.2.1. Compaction process record

The compaction process record is a number of tables in the database servers, which store the

historical data of multi-machine compaction process. It includes the trajectory point record, the strip boundary record, and the grid passes record (see Fig. 3(a)).

The trajectory point record is represented as a vector $P(n,t,C_p,N_p,V_p,A_p,F_p,l_p)$, where n,t,C_p are respectively roller ID, sampling time, and three-dimensional (3D) coordinates of the trajectory point $P_{n,t}$; and N_p,V_p,A_p,F_p,l_p are respectively roller passes, vehicle speed, amplitude, frequency, and overlap distance of roller *n*# from $t-\Delta t$ to t.

The strip boundary record stores the points that constitute the boundaries (i.e. $A_{n,t}B_{n,t}$、$C_{n,t}D_{n,t}$) of the compaction zone $\Omega(n,t)$ (see Fig. 3(f)). It provides spatial information about strip boundary for calculating the overlap distance. The stored data can be described as a vector $L(n,t,C_L,N_L,H_L)$, where n,t,C_L,N_L respectively represent the roller ID, sampling time, coordinates of boundary points, and roller passes corresponding to the compaction zone $\Omega(n,t)$. H_L is the orientation eigenvalue that equals either 1 or 2. $H_L=1$ indicates that the point is located on the upper strip boundary, i.e. $A_{n,t}B_{n,t}$; while $H_L=2$ indicates that the point is located on the lower strip boundary, i.e. $C_{n,t}D_{n,t}$ (see Fig. 3(f)). In this study, the "upper" orientation is defined as the left-hand side, when one faces the direction of increasing mileage.

The grid passes record uses the discrete grids to accumulate the roller passes at any location of the whole construction zone. The stored data can be described as a vector $G_k(C_k,N_k)$, where *k* is the code number of the grid, C_k is the coordinates of the grid center, and N_k is

the roller passes in grid *k*.

In each cycle period (Δt), the calculated compaction parameters (vehicle speed, roller passes, excitation force, and overlap distance) and other information (coordinates, roller ID, sampling time, and strip boundary layout) are updated in corresponding tables of the compaction process record.

5.2.2. Calculation of compaction zone

In Fig. 3(b), upon the receipt of the coordinate point $P_{n,t}$ from roller *n*# at time *t*, the precedent coordinate point $P_{n,t-\Delta t}$ is retrieved from the trajectory point record. Then the trajectory of roller *n*# from $t-\Delta t$ to t can be determined as $P_{n,t-\Delta t}P_{n,t}$ (see Fig. 3(f)). The compaction zone $\Omega(n,t)$ of roller *n*# from $t-\Delta t$ to t can be represented as a rectangle. The length of the rectangle is $P_{n,t-\Delta t}P_{n,t}$ and its width is the drum width $D(n)$ (see Fig. 3(f)). Therefore, the coordinates of the four vertexes (i.e. $A_{n,t}$, $B_{n,t}$, $C_{n,t}$, and $D_{n,t}$) of $\Omega(n,t)$ can be obtained with the known $D(n)$ and $P_{n,t-\Delta t}P_{n,t}$.

5.2.3. Calculation of vehicle speed

The average velocity between $t-\Delta t$ and t is used to represent the vehicle speed at time *t* (see Fig. 3(c)). Given two trajectory points $P_{n,t-\Delta t}(x_{n,t-\Delta t}, y_{n,t-\Delta t}, z_{n,t-\Delta t})$ and $P_{n,t}(x_{n,t}, y_{n,t}, z_{n,t})$, the speed of roller *n*# at time *t*, $v_{n,t}$, can be calculated using Eq. (1).

$$v_{n,t} = \frac{\sqrt{(x_{n,t}-x_{n,t-\Delta t})^2 + (y_{n,t}-y_{n,t-\Delta t})^2 + (z_{n,t}-z_{n,t-\Delta t})^2}}{\Delta t} \quad (1)$$

The calculated $v_{n,t}$, together with the sampling time *t*, roller ID *n*, and etc., is updated into the trajectory point record $P(n,t,C_p,N_p,V_p,A_p,F_p,l_p)$.

5.2.4. Calculation of roller passes

There are two types of roller passes defined in this study: the grid roller passes and the compaction zone roller passes (see Fig. 3(d)). Eq. (2) calculates the roller passes at a grid cell from a micro level.

$$N_k = \begin{cases} N_k + 1, & C_k \in \Omega(n,t) \\ N_k, & C_k \notin \Omega(n,t) \end{cases} \tag{2}$$

where, N_k is the roller passes at the grid G_k, with an initial value of zero. $C_k \in \Omega(n,t)$ means that the grid center C_k is inside the compaction zone $\Omega(n,t)$, while $C_k \notin \Omega(n,t)$ means it is outside the $\Omega(n,t)$.

The compaction zone roller passes reflects the macro-level roller passes that a certain roller is exerting. Due to the overlapping of adjacent strips, it is inevitable that different grids in the same $\Omega(n,t)$ have different roller passes N_k. Nevertheless, using the statistic method, the passes value that occupies the largest proportion in an $\Omega(n,t)$ can be determined based on the grid passes record $G_k(C_k,N_k)$. The obtained value is denoted by $N_{\Omega(n,t)}$, representing the roller passes of the overall compaction zone. The $N_{\Omega(n,t)}$ is updated to the relevant elements in $P(n,t,C_p,N_p,V_p,A_p,F_p,l_p)$ and $L(n,t,C_L,N_L,H_L)$ after calculation.

5.2.5. Calculation of overlap distance

The overlap distance refers to the overlapping width between adjacent compaction strips under the same roller passes (see Fig. 4(a)). The calculation process is detailed below (see Fig. 3(e)).

(1) Boundary points retrieval

The strip boundary points (blue dots in Fig. 4(b)) with the roller passes of $N_{\Omega(n,t)}$ that are inside the compaction zone $\Omega(n,t)$ are identified by searching the vector $L(n,t,C_L,N_L,H_L)$. The existence of point set $\left\{C_L \middle| C_L \in \Omega(n,t), N_L = N_{\Omega(n,t)}\right\}$ leads to the boundary points fitting mentioned in the next step. If the point set is empty, the anomaly identification algorithm will be initialized.

(2) Boundary points fitting

Due to positioning errors and the factor of driving skills, the roller trajectories are not smooth; and thus the recorded boundary points are not on a straight line (see Fig. 4(b)). To calculate the overlap distance, the point set $\left\{C_L \middle| C_L \in \Omega(n,t), N_L = N_{\Omega(n,t)}\right\}$ needs to be fitted to a straight line that represents the strip boundary. The least square method is used for linear fitting. The boundary point is denoted by (x_L, y_L); and the mathematic formula of boundary fitting is shown in Eq. (3).

$$\begin{cases} \text{obtain:} \quad y = f(x) = ax + b \\ \text{s.t.} \quad s = \sum_{M} [y_L - f(x_L)]^2 \rightarrow \min \end{cases} \tag{3}$$

where, M is the point set $\left\{C_L \middle| C_L \in \Omega(n,t), N_L = N_{\Omega(n,t)}\right\}$. By setting the partial derivatives of s with respect to a and b equal to zeros, the values of a and b can be solved.

(3) Overlap distance calculation

For point set $\left\{C_L \middle| C_L \in \Omega(n,t), N_L = N_{\Omega(n,t)}\right\}$, if the orientation eigenvalue $H_L = 1$, the current compaction zone is overlapped with the upper boundary of the adjacent strip. In this circumstance (see Fig. 4(c)), the distances of $\mathrm{C}_{n,t}$ and $\mathrm{D}_{n,t}$ to the straight line $y = ax + b$ are calculated, which are respectively denoted by $l_{n1,t}$ and $l_{n2,t}$. Then the overlap distance of roller *n*# at time *t* can be obtained as the average of $l_{n1,t}$ and $l_{n2,t}$, namely, $l_{n,t} = (l_{n1,t} + l_{n2,t})/2$. If $H_L = 2$, the overlap distance is calculated by averaging the distance of $\mathrm{A}_{n,t}$ and $\mathrm{B}_{n,t}$ to the straight line $y = ax + b$.

(4) Update of compaction process record

The element l_p in the trajectory point record is updated using the calculated $l_{n,t}$ for subsequent data query and data analysis. In addition, the constitutive points (e.g. $\mathrm{A}_{n,t}$, $\mathrm{B}_{n,t}$, and interpolated points) of the strip boundaries of compaction zone $\Omega(n,t)$ are updated in the strip boundary record.

5.3. Procedure for collaborative compaction control

Fig. 5 presents a procedure for collaborative and real-time control of compaction sequence, overlap distance, vehicle speed, excitation force, and roller passes with multi-roller operations. With the hardware mounted on the rollers, the multi-machine operation information is collected in real time. The collected data are then used to calculate compaction parameters on the remote servers. Next, the calculated compaction parameters are compared

with pre-set compaction criteria to identify the unqualified compaction efforts. If there are anomalies, warning messages will be automatically generated and fed back to the in-situ control module (ICM) and the monitoring terminal (MOT).

A three-layer inspection system is created to ensure the timely adjustment of unqualified compaction efforts. First, when receiving the monitoring data from the remote servers, roller operators adjust compaction efforts to meet the construction requirements. Second, if the anomalies are not rectified timely or the actions of different rollers contradict each other, in-situ supervisors will intervene to coordinate the adjustment efforts. Third, if the anomalies are still not rectified, the administrative personnel who monitor the overall compaction process with the monitoring terminal can directly send adjustment instructions to the field supervisors. Anomaly identification is critical for the feedback control. Thus, the specific methods for anomaly recognition are detailed below.

5.3.1. Anomaly recognition of compaction sequence

$R_s(x)$ is the control criterion for compaction sequence, which represents a set of IDs of the assigned rollers for rolling the zone in the pass of x. If the ID of current roller n satisfies $n \in R_s(N_{\Omega(n,t)})$, the compaction sequence of roller n# at time t is compliant; if not, the compaction sequence is not compliant, and a warning is generated.

5.3.2. Anomaly recognition of vehicle speed

$V_s(x)$ is the control criterion for vehicle speed, which represents the normal range of vehicle

speed for rolling the zone in the pass of *x*. If $v_{n,t} \in V_s(N_{\Omega(n,t)})$ holds, the vehicle speed of roller *n#* at time *t* is compliant; if not, the vehicle speed is not compliant, and a warning is generated.

5.3.3. Anomaly recognition of excitation force

The excitation force is reflected by the roller vibration frequency and amplitude, which are separately obtained by conducting Fast Fourier Transform (FFT) and frequency-domain integral to the collected acceleration signal. The frequency and amplitude of roller *n#* at time *t* are respectively denoted by $f_{n,t}$ and $A_{n,t}$. $F_s(x)$ and $A_s(x)$ are the control criteria for excitation force, which respectively represent the normal range of vibration frequency and amplitude for rolling the zone in the pass of *x*. If $f_{n,t} \in F_s(N_{\Omega(n,t)})$ and $A_{n,t} \in A_s(N_{\Omega(n,t)})$ hold at the same time, the excitation force of roller *n#* at time *t* is compliant; if not, the excitation force is not compliant, and a warning is generated.

5.3.4. Anomaly recognition of overlap distance

If there is no strip boundary point C_L within $\Omega(n,t)$ that makes $\left\{C_L \middle| C_L \in \Omega(n,t), N_L = N_{\Omega(n,t)}\right\}$ hold, it means that the current compaction zone is not overlapped with the adjacent strip, and hence the roller operation status is not compliant. If the eligible C_L exists, the overlap distance $l_{n,t}$ is compared with the control criterion $l_s(x)$. If $l_{n,t} \in l_s(N_{\Omega(n,t)})$, the overlap distance of roller *n#* at time *t* is compliant; if $l_{n,t} \notin l_s(N_{\Omega(n,t)})$, the overlap distance is not compliant.

401 *5.3.5. Anomaly recognition of roller passes*

402 After finishing the compaction of a construction zone, statistical analysis is performed to the
403 roller passes of all the grids in the work unit. When Eq. (4) holds, roller passes of the
404 construction zone is compliant; otherwise, the roller passes is not compliant, and extra
405 compaction efforts should be exerted to the under-compacted areas.

406
$$\frac{\sum_{(k)} g\left(\sum_{\gamma(f)}\sum_{\alpha(n)} N_{k,n,f} \geq N_s\right)}{\sum_{(k)} g(N_k \geq 0)} \geq \delta \tag{4}$$

407 where, $g(x)$ is a discrimination function, and the function value equals 1 when the condition
408 denoted by x holds; otherwise, the function value equals 0. k and N_k are respectively the
409 code number and the total roller passes of grid G_k. $\alpha(n)$ and $\gamma(f)$ are respectively a
410 given set of roller ID n and vibration status f; vibration status f is either 0 or 1, which
411 respectively represents static mode or vibration mode. $N_{k,n,f}$ is the roller passes of grid G_k
412 under roller n# with f status. N_s is the standard roller passes under a certain working
413 condition, e.g. static compaction and initial rolling. δ is the pre-set threshold value, which
414 is usually a number over 90%. Using Eq. (4), the qualification rate of roller passes under
415 different working conditions (e.g. static compaction, initial rolling, and the total roller passes)
416 can be evaluated.

417

418 **6. Field experiments**

419 A compaction process monitoring system is developed (a system interface shown in Fig. 6)
420 and applied in an expressway project that is under construction in Tianjin, China, in July,
421 2016. The demonstration section is the bottom surface layer of asphalt pavement, which is

paved with 12 cm of asphalt treated base mixture (ATB).

6.1. Compaction scheme

The machinery used in the project includes 2 rubber tyre rollers, XCMG XP302, 3 double-drum vibratory rollers from DYNAPAC, CC624HF, and 2 double-drum vibratory rollers from Ingersoll Rand, DD-125. The detailed compaction scheme is described below.

(1) Initial rolling. This process is conducted by DYNAPAC CC624HF with low speed and static mode for 4 times, and overlap is not required.

(2) Repeated rolling. The pavement material is first compacted by rubber tyre rollers, XCMG XP302, with medium speed and 60cm of overlap distance for 2 times; then the compaction is conducted by DYNAPAC CC624HF for 6 times, with medium speed, high vibration frequency and large amplitude, and 20cm of overlap distance.

(3) Final rolling. This process is performed by Ingersoll Rand DD-125 with static mode and no overlap requirement for 4 times.

6.2. Compaction process control

6.2.1. Control of compaction sequence

The two XCMG XP302, three DYNAPAC CC624HF, and two Ingersoll Rand DD-125 are separately coded with ID number 1#~7#. A control criterion for compaction sequence is developed as Table 2.

Fig. 7 shows the graphical reports of roller distribution for a road section, which can be used to evaluate the compliance of compaction sequence. In Fig. 7(a), the color blocks representing roller 3# and roller 4# distribute symmetrically along the central axis of the pavement, which is consistent with the compaction scheme, reflecting that the rolling sequence is executed correctly for the 1st pass. For the 5th pass, the compaction should be conducted by the XCMG XP302 (roller 1# and roller 2#) according the scheme. However, Fig. 7(b) presents an unqualified region marked by a shadow area, which is caused by the incorrect execution of rolling sequence by roller 4#.

6.2.2. Control of vehicle speed, excitation force and roller passes

The real-time velocity and excitation force of each roller are displayed on the interface of the monitoring terminal (MOT) (see Fig. 6). Fig. 8 presents the graphical report of compaction trajectory for a road section, in which the over-speed compaction and unqualified excitation force output are highlighted in yellow and red respectively. Fig. 9(a), 9(b), and 9(c) respectively show the graphical reports of total roller passes, vibratory roller passes and static roller passes for the road section, with the qualification rate of 96.25%, 97.02% and 95.98%.

6.2.3. Accuracy and control of overlap distance

An experiment is carried out to verify the algorithm for overlap distance calculation. There are two overlapping groups on a 50m experimental section. Group 1# is overlapped by strip 1 and strip 2, with the overlap distance of 20cm; Group 2# is overlapped by strip 2 and strip 3, with the overlap distance of 30cm. A roller is assigned to move along the designated

boundaries which are highlighted on the pavement surface. Afterwards, the calculated overlap distance is compared with the pre-set standard value, and the results are shown in Fig. 10. The calculation error of overlap distance is less than ±2.5cm, mainly resulting from the precision of RTK positioning (1-3cm). The largest relative error is 11.5%, which meets the requirement for project application. Warnings of overlap distance were issued frequently during the construction, which is caused by the high requirements of the operators' driving skills to control overlap distance.

6.3. Results analysis of compaction process control

To validate the effectiveness of the proposed method, the compaction quality after system application is evaluated from the perspective of compactness, roughness, and uniformity, as is shown in Table 3. Compactness is indicated by density, and totally 25 samples scattered around the pilot section are collected by non-nuclear density gauge; roughness is measured by the continuous evenness device, which is then transformed into international roughness index (IRI), and 10 samples are collected in total; uniformity is assessed by the semivariogram analysis for CMV of the last pass of repeated rolling [23-25, 28], and three 100-meters-long sections are selected as the analyzed objects from different parts of the pilot section. In case of the influence of data anomalies in certain areas, locations of all the samples are selected randomly.

In terms of compactness, the average density (2.533 g/cm^3) of the sampling points accounts for 96.5% of the maximum theoretical density, which is greater than the standard value 94%.

In terms of roughness, the average IRI of the 10 sampling points is 1.6 m/km, which is less than the upper control limit 2.0 m/km. In terms of uniformity, literature [26, 27] points out that the lower the “sill” is and/or the larger the “range” is, the better uniformity is achieved, while the opposite indicates a less uniform compaction. Fig. 11 depicts the distribution graphs of CMV kriging interpolation and the semivariograms of CMV for three 100m road sections. The average values of “sill” and “range” of the fitted models are respectively 5.88 and 17.03, which indicates that a relatively uniform compaction is achieved.

These results indicate that the demonstration section is well-compacted, which is probably related to the real-time control of the compaction process. With the application of the system, the key compaction parameters (i.e. rolling sequence, roller passes, vehicle speed, excitation force, and overlap distance) are put under strict control, and any inappropriate compaction effort of multi-rollers can be identified, tracked, and rectified in real time. Hence, the compaction scheme is followed strictly, leading to better compaction quality.

However, it should be noted that this study is subject to several limitations. First, despite the effectiveness demonstrated by the pilot project, the long-term influence and applicability of the proposed method on different types of asphalt pavement still need further investigation by conducting more field application. Second, the prototype system may generate false warnings where the construction condition is complicated (e.g. interface between two rolling section, retracing area for roller movement). In practice, this problem can be minimized by setting a threshold of duration before issuing a warning.

7. Conclusion and prospect

The asphalt pavement compaction aims to achieve good compactness, roughness, and uniformity. In this paper, the collaborative and real-time control methods of compaction sequence, overlap distance, roller passes, vehicle speed, and excitation force are investigated for the multi-machine situation. The proposed solution for multi-machine compaction monitoring, algorithms for compaction parameters calculation, and procedure for collaborative compaction control respectively address the issues of data communication, data analytics, and feedback control from the perspective of a cyber-physical system. The real-world case study in Tianjin, China, indicates that the proposed methods can effectively control the compaction process, resulting in better compactness, roughness, and uniformity.

In the future, current compaction control methods, characterized by single-roller and human-involved, will evolve into a collaborative and automatic cyber-physical system. The authors' vision is that, the pavement's compactness, roughness, and uniformity are assessed in real time during the compaction process based on the collected multi-machine information, and then the operation scheme, compaction efforts (vehicle speed, frequency, and amplitude), and the roller assignment are dynamically adjusted to attain the compaction objectives. To achieve this, further researches should focus on two aspects. First, the evaluation model of compaction quality needs to be investigated by considering the compactness, roughness, and uniformity in a holistic manner. Second, the mechanism for controlling onsite machines remotely via cyberspace should be explored to automate the feedback control process.

Acknowledgements

This research was supported by the National Key Research and Development Program of China (No. 2017YFC0405100), the Foundation for Innovative Research Groups of the National Natural Science Foundation of China (No.51621092), and the National Natural Science Foundation of China (No.51679164).

References

[1] Ministry of Transport of the People's Republic of China, JTG F40-2004 Technical Specification for Construction of Highway Asphalt Pavements, 2004, China Communic-ations Press: Beijing, China (in Chinese), http://xueshu.baidu.com/s?wd=paperuri%3A%28f3b4ea1c69628a4688322db2da04556c%29&filter=sc_long_sign&tn=SE_xueshusource_2kduw22v&sc_vurl=http%3A%2F%2Fwww.docin.com%2Fp-1462017.html&ie=utf-8&sc_us=6747103654208480011 (Jul. 7, 2018).

[2] R. Anderegg, K. Kaufmann, Intelligent compaction with vibratory rollers - Feedback control systems in automatic compaction and compaction control, Soil Mechanics 1868 (2004) 124-134, https://doi.org/10.3141/1868-13.

[3] E. Kassem, W. Liu, T. Scullion, et al., Development of compaction monitoring system for asphalt pavements, Construction and Building Materials, 96 (2015) 334-345, https://doi.org/10.1016/j.conbuildmat.2015.07.041.

[4] Q. Xu, G.K. Chang, Adaptive quality control and acceptance of pavement material density for intelligent road construction, Automation in Construction 62 (2016) 78-88, https://doi.org/10.1016/j.autcon.2015.11.004.

[5] D.H. Liu, M. Lin, S. Li, Real-time quality monitoring and control of highway compaction, Automation in Construction 62 (2016) 114-123, https://doi.org/10.1016/j.autcon.2015.11.007.

[6] D.H. Liu, J. Sun, D.H. Zhong, et al., Compaction quality control of earth-rock dam construction using real-time field operation data, Journal of Construction Engineering and Management 138 (9) (2012) 1085-1094, https://doi.org/10.1061/(asce)co.1943-7862.0000510.

[7] National Academies of Sciences, Engineering, and Medicine, Intelligent Soil Compaction Systems, 2010, The National Academies Press: Washington, DC., America, https://doi.org/10.17226/22922.

[8] M.A. Mooney, R.V. Rinehart, Field monitoring of roller vibration during compaction of subgrade soil, Journal of Geotechnical and Geoenvironmental Engineering 133 (3) (2007) 257-265, https://doi.org/10.1061/(asce)1090-0241(2007)133:3(257).

[9] J. Scherocman, S. Rakowski, K. Uchiyama, Intelligent compaction, does it exist?, in the Annual Conference—Canadian Technical Asphalt Association, 2007: Canada, https://www.researchgate.net/publication/268403022_Intelligent_Compaction_Does_It_Exist (Jul. 7, 2018).

[10] A.G. Correia, H. Brandl, Geotechnics for Roads, Rail Tracks, and Earth Structures , Swets & Zeitlinger Publishers, Lisse, Netherlands, 2001, ISBN 9026518447.

[11] K. Kaufmann, R. Anderegg, 3D-construction applications III: GPS-based compacti on t-echnology, in Proc., 1st Int. Conf. on Machine Control & Guidance, 2008: ETH Zurich, Switzerland, https://www.researchgate.net/publication/288950640_GPS-based_Compaction_Technology (Jul. 7, 2018).

[12] R.V. Rinehart, M.A. Mooney, Instrumentation of a roller compactor to monitor vi bration behavior during earthwork compaction, Automation in Construction 17 (2) (2008) 144-150, https://doi.org/10.1016/j.autcon.2006.12.006.

[13] M.A. Mooney, P.B. Gorman, J.N. Gonzalez, Vibration-based health monitoring of earth structures, Structural Health Monitoring-an International Journal 4 (2) (2005) 137-152, https://doi.org/10.1177/1475921705049759.

[14] M.J. Thompson, D.J. White, Estimating compaction of cohesive soils from machine drive power, Journal of Geotechnical and Geoenvironmental Engineering 134 (12) (2008) 1771-1777, https://doi.org/10.1061/(asce)1090-0241(2008)134:12(1771).

[15] L. Petersen, Continuous compaction control MnROAD demonstration, Final report submitted to Mn/DOT, 2005, Minnesota DOT, Office of Research Services: Minnesota, America, http://www.dot.state.mn.us/research/TS/2005/200507.pdf (Jul. 7, 2018).

[16] M. Thompson, D. White, H. Gieselman, et al., Variable feedback control intelligent compaction to evaluate subgrade and granular pavement Layers—Field study at Minnesota US 14, in Transportation Research Board 87th Annual Meeting, 2008: Washington, D.C., America, http://www.trb.org/main/blurbs/162019.aspx (Jul. 7, 2018).

[17] C.L. Meehan, D.V. Cacciola, F.S. Tehrani, et al., Assessing soil compaction using continuous compaction control and location-specific in situ tests, Automation in Construction 73 (2017) 31-44, https://doi.org/10.1016/j.autcon.2016.08.017.

[18] B.H. Shi, Y.M. Zhang, T. Sun, et al., Analysis and discussion on impact factor to asphalt pavement roughness of airport, Advanced Materials Research 779-780 (2013) 510-515, https://doi.org/10.4028/www.scientific.net/amr.779-780.510.

[19] K.Y. Chen, M.M. Lu, X.P. Fan, et al., Road condition monitoring using on-board three-axis accelerometer and GPS sensor, in 2011 6th International ICST Conference on Communications and Networking in China, 2011: Harbin, China, https://doi.org/10.1109/chinacom.2011.6158308.

[20] A. Loizos, C. Plati, An alternative approach to pavement roughness evaluation, International Journal of Pavement Engineering 9 (1) (2008) 69-78, https://doi.org/10.1080/10298430600949894.

[21] D.H. Liu, Y. Wu, S. Li, et al., A real-time monitoring system for lift-thickness control in highway construction, Automation in Construction 63 (2016) 27-36, https://doi.org/10.1016/j.autcon.2015.12.004.

[22] R. Walters, E. Jaselskis, J.Z. Zhang, et al., Using scanning lasers to determine the thickness of concrete pavement, Journal of Construction Engineering and Management 134 (8) (2008) 583-591, https://doi.org/10.1061/(asce)0733-9364(2008)134:8(583).

[23] P.K.R. Vennapusa, D.J. White, M.D. Morris, Geostatistical analysis for spatially r efere-nced roller-integrated compaction measurements, Journal of Geotechnical an d Geoenvi-ronmental Engineering 136 (6) (2010) 813-822, https://doi.org/10.1061/(asce)gt.1943-5606.0000285.

[24] Q.W. Xu, G.K. Chang, Experimental and numerical study of asphalt material geo spatial heterogeneity with intelligent compaction technology on roads, Construction and Buildi-ng Materials 72 (2014) 189-198, https://doi.org/10.1016/j.conbuildmat.2014.09.003.

[25] Q.W. Xu, G.K. Chang, V.L. Gallivan, et al., Influences of intelligent compaction uniformity on pavement performances of hot mix asphalt, Construction and Building Materials 30 (2012) 746-752, https://doi.org/10.1016/j.conbuildmat.2011.12.082.

[26] D. Zhong, B. Cui, D. Liu, et al., Theoretical research on construction quality real -time monitoring and system integration of core rockfill dam, Science in China Series E: Tec-hnological Sciences 52 (11) (2009) 3406-12, https://doi.org/10.1007/s11431-009-0343-6.

[27] D. Zhong, D. Liu, B. Cui, Real-time compaction quality monitoring of high core rockfill dam, Science in China Series E: Technological Sciences 54 (7) (2011) 19 06-13, https://doi.org/10.1007/s11431-011-4429-6.

[28] Q.W. Xu, G.K. Chang, Evaluation of intelligent compaction for asphalt materials, Automation in Construction 30 (2013) 104-112, https://doi.org/10.1016/j.autcon.2012.11.015.

[29] E.H. Isaaks, R.M. Srivastava, An Introduction to Applied Geostatistics, Oxford Un iv.Press, New York, 1989, ISBN 0195050126.

[30] I. Clark, W. Harper, Practical Geostatistics, 3rd edition Ecosse North America LL C, Columbus, OH, 2002, ISBN 0970331703.

639 # Tables

640 **Table 1.** Findings about ICMV's correlation with spot tests in previous studies.

Literatures	ICMV	Related results
Mooney et al. [12, 13]	CMV CCV THD	✓ The correlations improve significantly if the underlying materials are stiff
Thompson and White [14]	MDP	✓ Statistical averaging of data improves the prediction of compaction parameters. ✓ Incorporating moisture content in multiple regression models improves correlation. ✓ The influence depth may affect the value of MDP.
Correia et al. [10] and Petersen [15]	E_{vib}	✓ Correia et al. [10] obtain a linear correlation with $R^2 > 0.9$ while Petersen [15] found poor correlations between E_{vib} and spot-test.
Thompson et al. [16]	k_B	✓ k_B has a good correlation with PLT (plate load test) moduli with $R^2=0.9$, while R^2 was relatively small (0.3 ~ 0.61) for correlations with other spot test measurements. ✓ The strength of correlation depends heavily on the range of values over which the measurements are taken.
Meehan et al. [17]	CMV MDP	✓ Using the average value of test data to do the correlation analysis can dramatically improve R^2. ✓ Multivariate regression analysis can obtain a better R^2 compared with univariate regression analysis.

641

642 **Table 2.** Control criterion for compaction sequence.

Pass	1~4	5~6	7~12	13~16
Roller ID	{3#,4#,5#}	{1#,2#}	{3#,4#,5#}	{6#,7#}

643

644 **Table 3.** Compaction quality evaluation after system application.

Compactness			Roughness		Uniformity		
Max theoretical density (g/cm^3)	Sample number	Average density (g/cm^3)	Sample number	Average IRI (m/km)	Sample number	Average Sill	Average Range (m)
2.626	25	2.533	10	1.6	3	5.88	17.03

645

646 # Figures

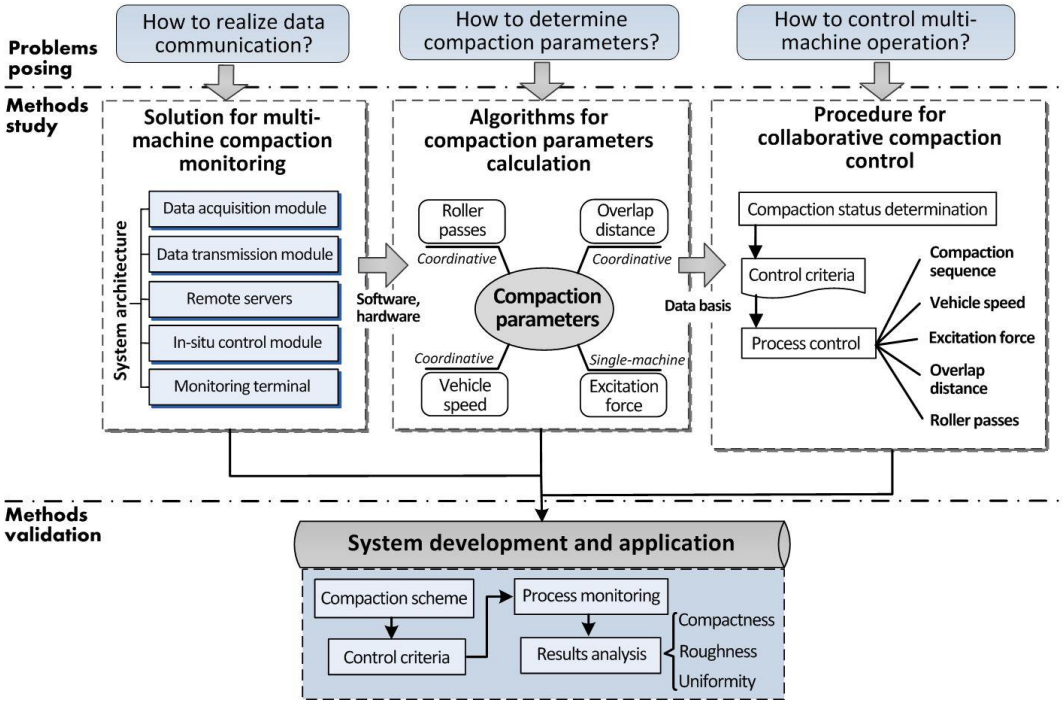

647

648 **Fig.1.** Research framework.

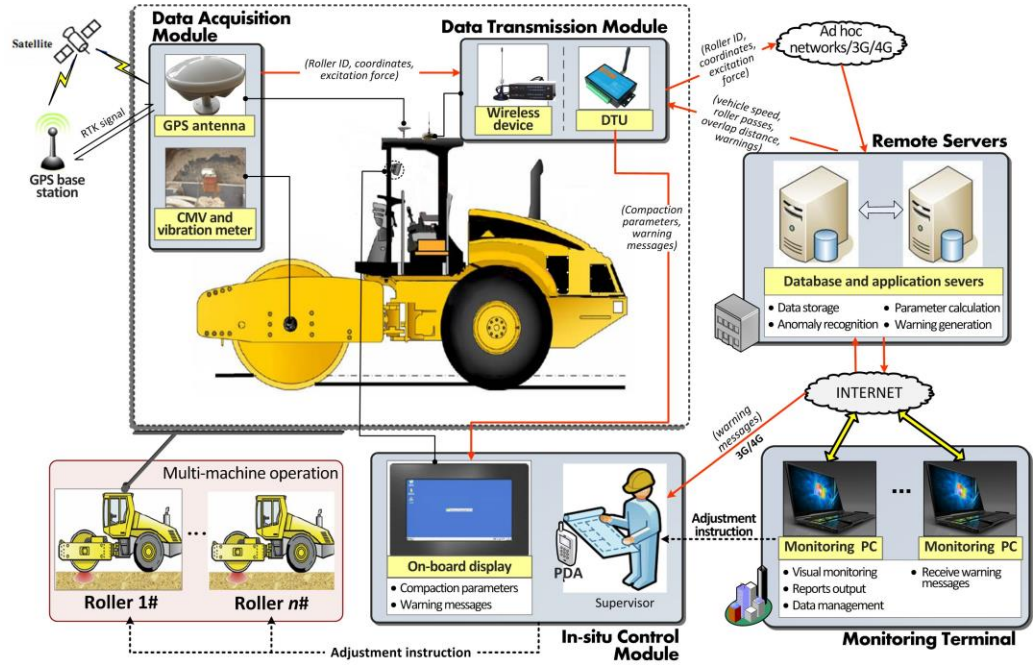

649

650 **Fig.2.** Overall architecture of multi-machine compaction process monitoring.

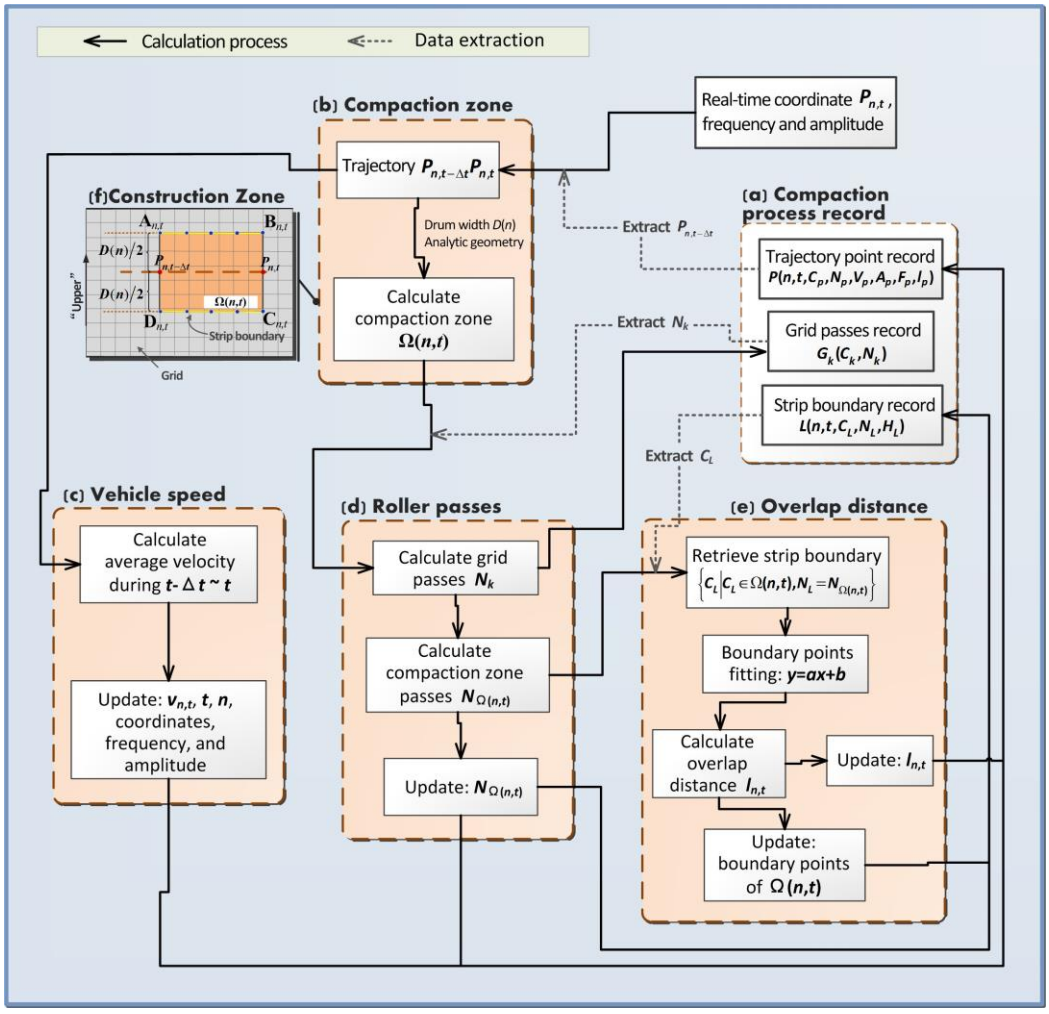

Fig.3. Flowchart of compaction parameters calculation.

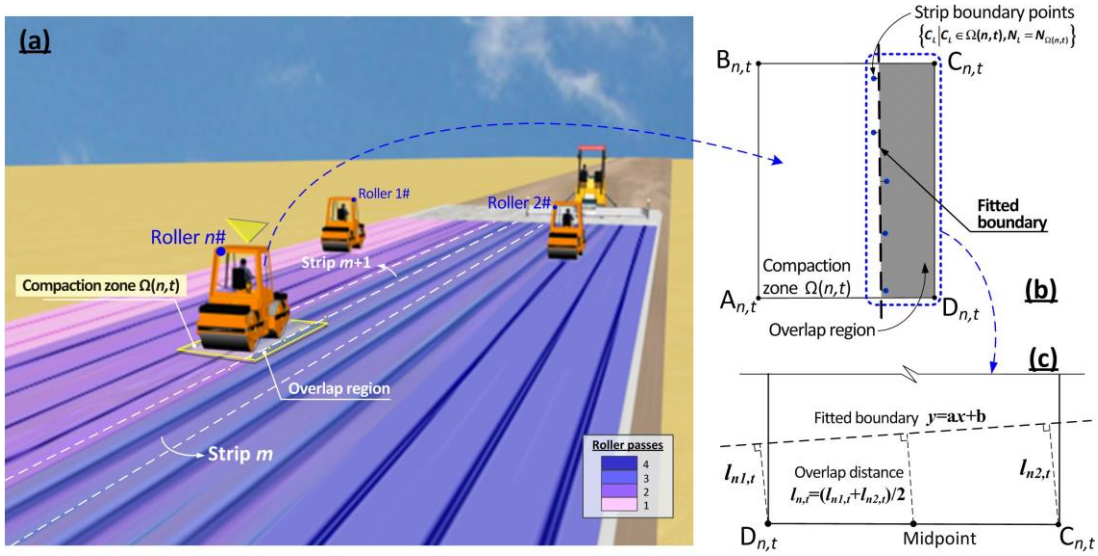

Fig.4. Calculation principles of overlap distance: (a) Overall layout of strips overlap; (b) Diagram of boundary points fitting; (c) Geometric model for overlap distance calculation.

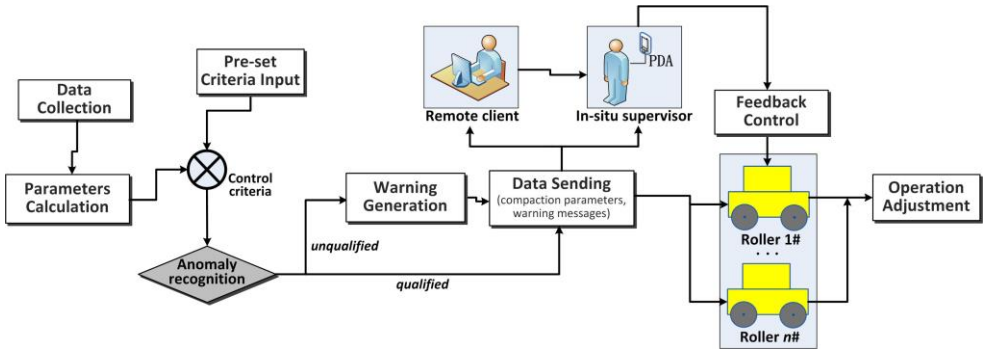

Fig.5. Procedure for collaborative compaction control.

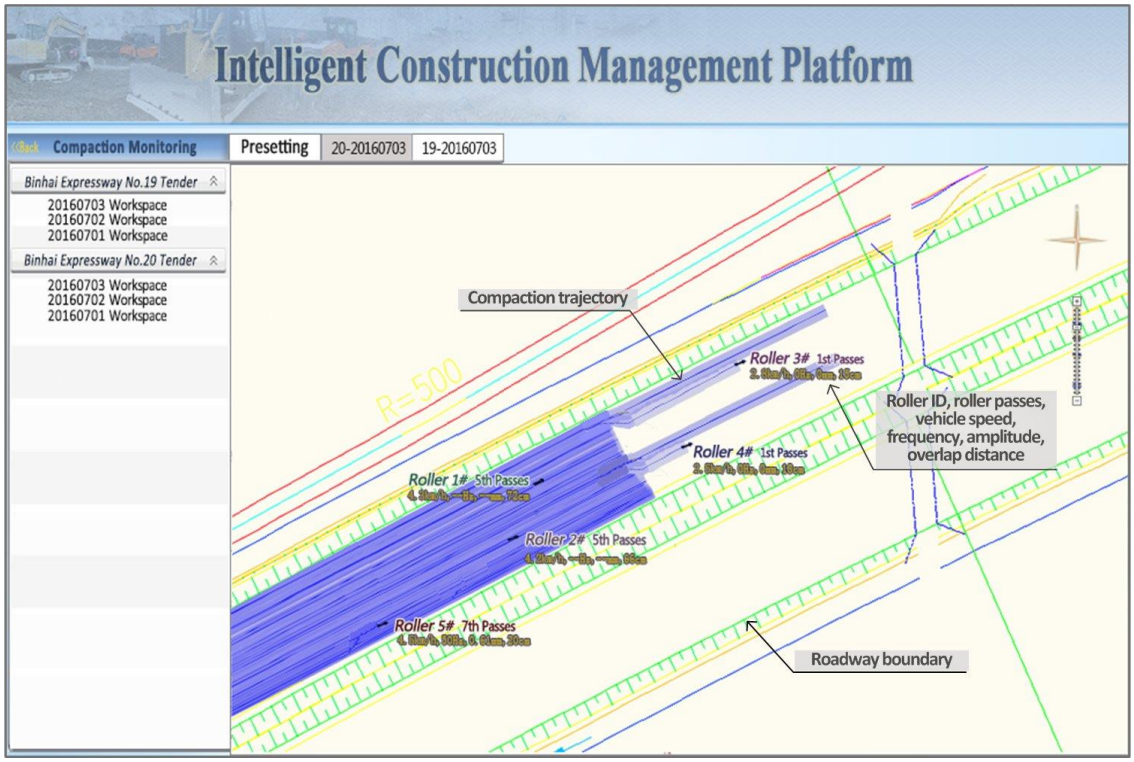

Fig.6. Screenshot of the monitoring terminal.

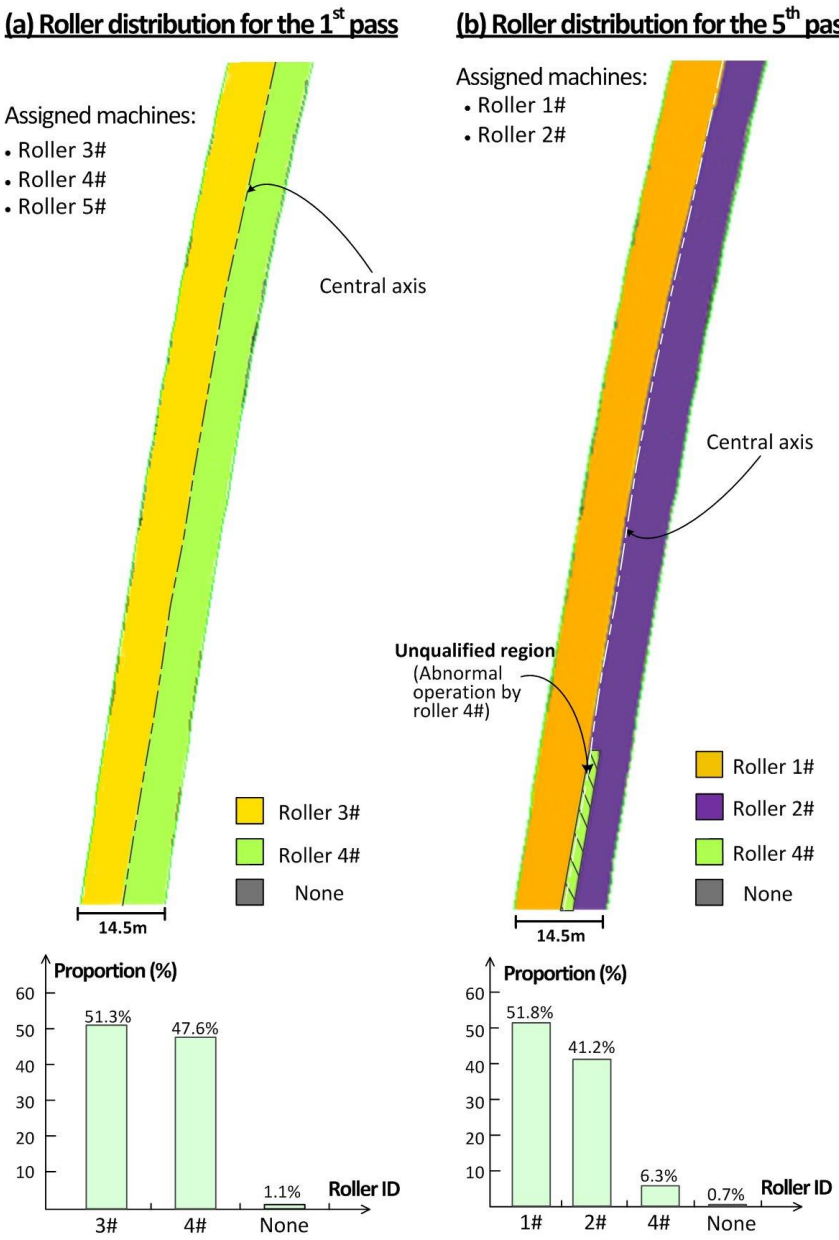

660

661 **Fig.7.** Graphical reports of roller distribution for section K102+900~K103+050.

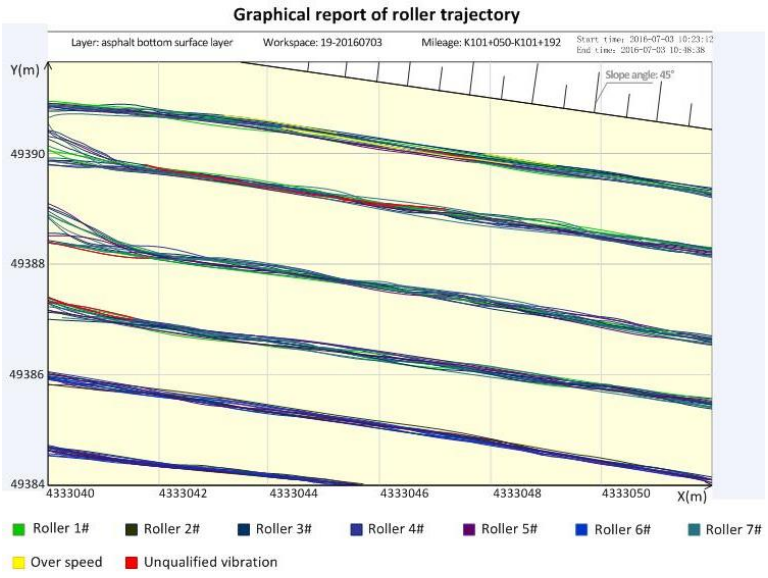

662

663 **Fig.8.** Graphical report of roller trajectory for section K101+050~K101+192.

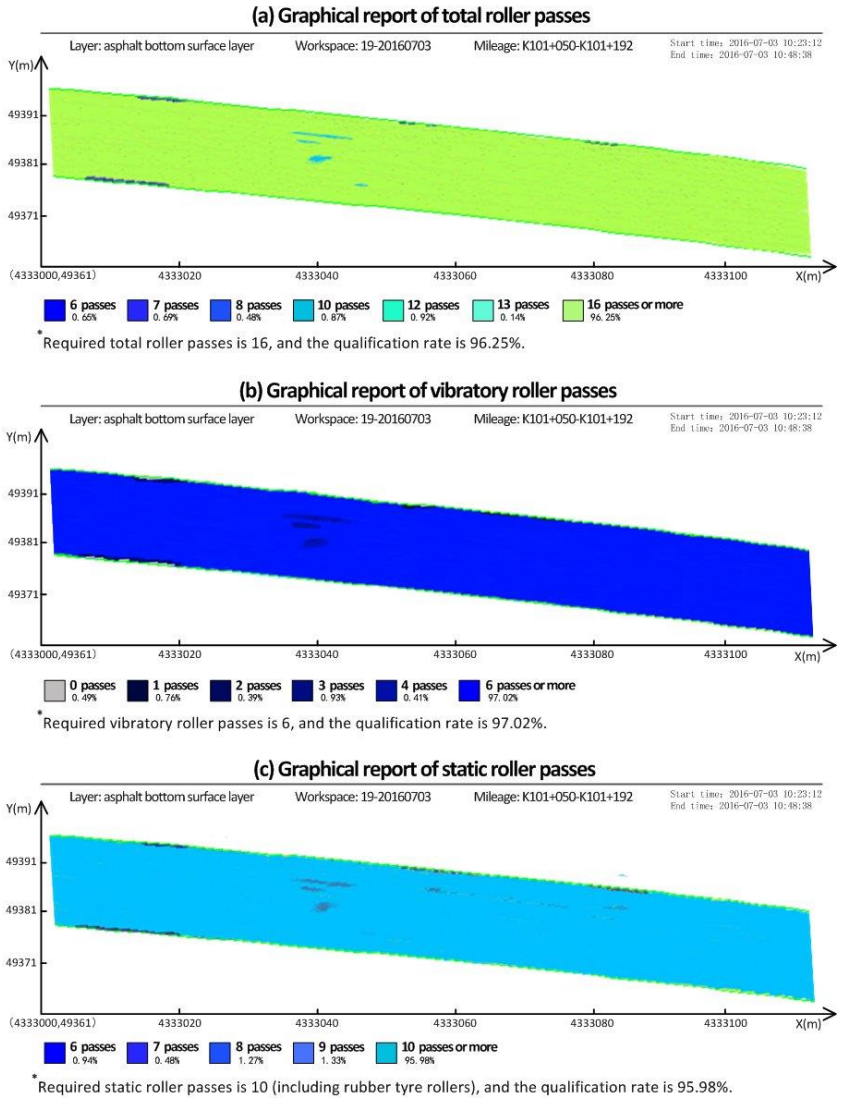

664

665 **Fig.9.** Graphical reports of roller passes for section K101+050~K101+192.

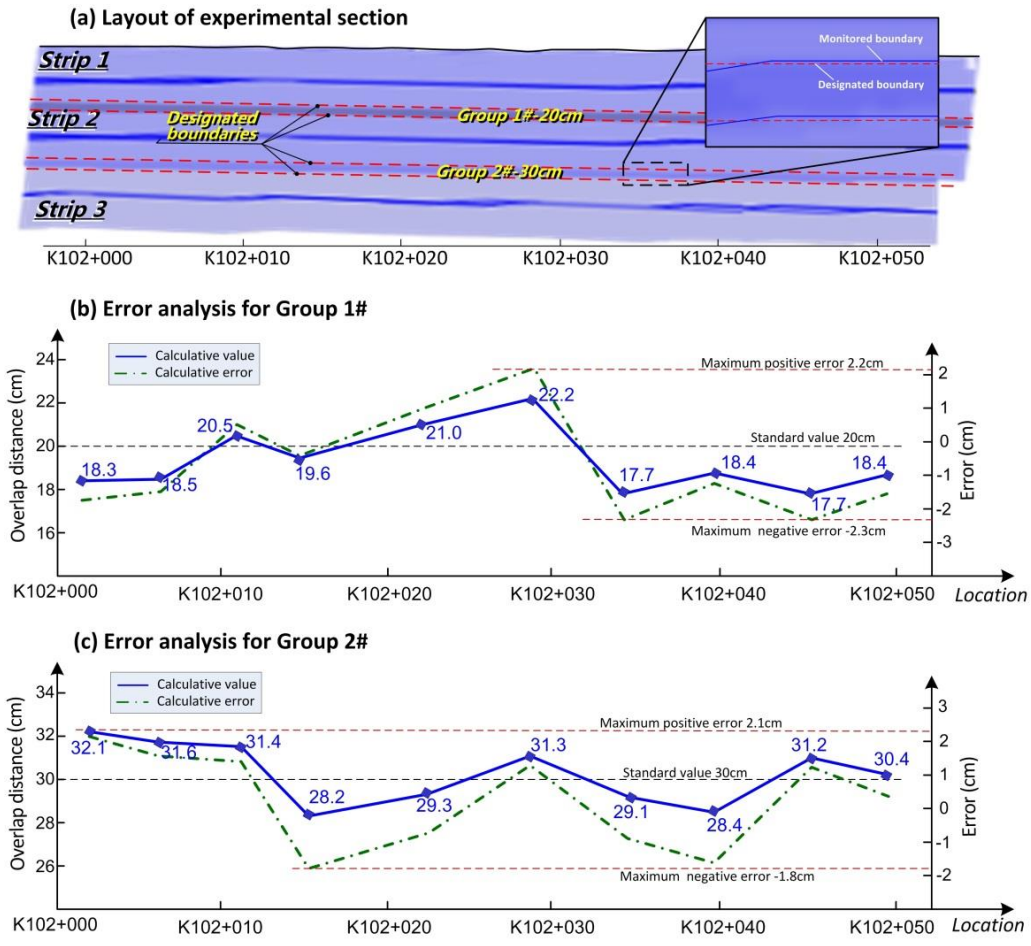

666

667 **Fig.10.** Error analysis for overlap distance calculation.

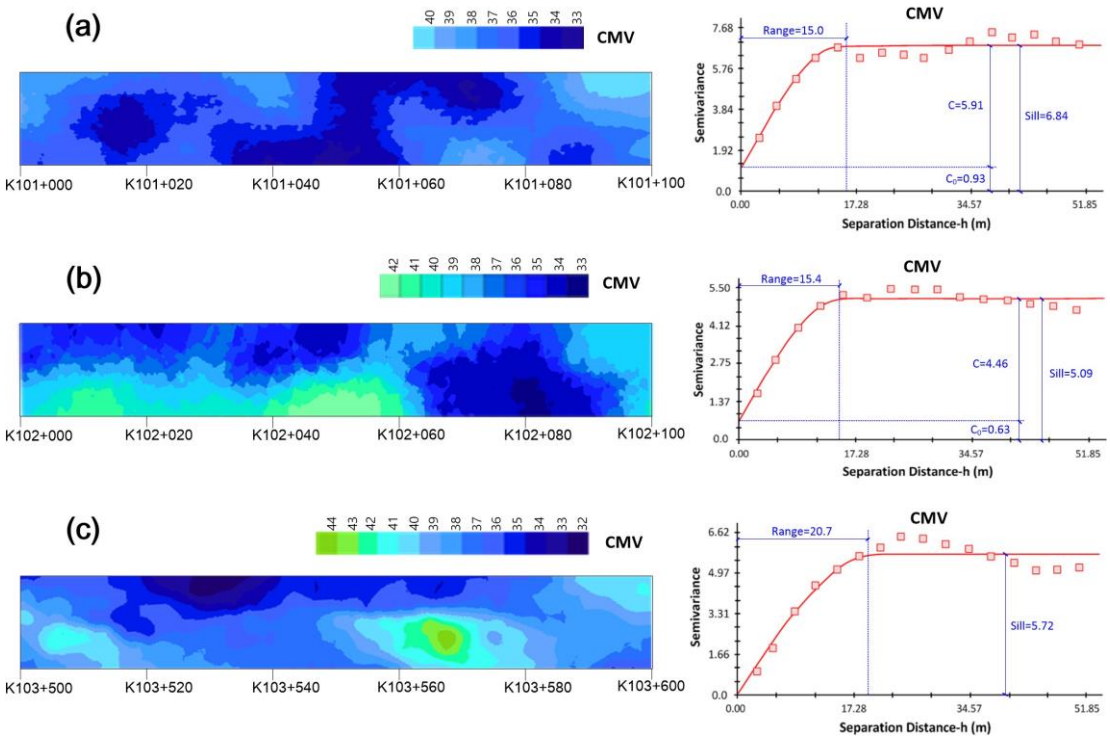

668

669 **Fig.11.** CMV kriging interpolation and semivariogram for section (a) K101+000~K101+100,

670 (b) K102+000~K102+100, and (c) K103+500~K103+600.